HYDROACOUSTIC PROPAGATION THROUGH THE ANTARCTIC CONVERGENCE ZONE: STUDY OF ERRORS IN YIELD AND LOCATION ESTIMATES FOR EXPLOSIVE CHARGES

C. de Groot-Hedlin[1], Donna K. Blackman[1], and C. Scott Jenkins[2]

Scripps Institution of Oceanography (SIO), University of California at San Diego[1]
Naval Surface Warfare Center, Indian Head Division (IHDIV)[2]

ABSTRACT

A series of small calibration shots was conducted in late December 2006, along a transect from New Zealand to Antarctica in order to document the differences in spectral characteristics, transmission loss, travel-time, and azimuth both observed and predicted using propagation models typical for nuclear monitoring. The high gradients in ocean temperature and salinity that characterize the Antarctic Convergence Zone (ACZ) are expected to alter the propagation path, and the commonly rough sea surface is likely to scatter significant energy from sources south of ~53°S, where the sound channel breaches the surface. Seasonal variability in the ACZ makes it difficult to model such effects accurately at all times, so our experiment was designed to determine the scale of error introduced by such uncertainty in structure. Depth charges, set to trigger at 300, 460, and 600 m, were deployed at 6 stations between 54°S and 63°S. The International Monitoring System (IMS) hydroacoustic station off Cape Leeuwin, Australia, recorded shots from all but one site. Macquarie Ridge probably blocked that source area. Several shots were also recorded at the Diego Garcia and Juan Fernandez IMS stations. This new data set will be characterized in terms of source-receiver transmission loss and spectral characteristics, used to infer source yield, as well as source location errors. Preliminary analysis of arrivals at IMS hydroacoustic stations in the Indian Ocean indicates that the time duration of each arrival depends on source location, and not on source depth or size. Conversely, the spectral content of the signals depends on source depth and charge size, but not on the source location.

OBJECTIVES

Our objectives were to conduct a series of calibration shots within and to the south of the ACZ that would generate acoustic signals at frequencies f>30 Hz and to analyze the signals recorded at hydrophone stations operated by the IMS. The overall goal was to compare observed source-receiver travel times to the IMS hydrophone stations to those predicted by numerical models for paths crossing the Antarctic convergence zone and to use results to determine the accuracy to which sources may be located within the ACZ. A second objective was to determine the accuracy of source yield estimates for explosive sources within the ACZ. A calibration experiment was needed because ocean temperature and salinity gradients within the southern ocean are not sufficiently well characterized to predict how travel times may be affected by seasonal and climactic variations.

Acoustic travel times vary seasonally because the upper ocean is warmed during summer and cools in winter, and sound travels faster in warmer water than in cold water. This seasonal variation in travel times has been observed in the Acoustic Thermometry of Ocean Climate (ATOC) experiment (Dushaw et al., 1999). Variability in travel times is particularly pronounced at high northern latitudes, where seasonal temperature changes may extend to the sound channel axis (Dushaw et al., 1999), and is expected to be significant in the southern ocean as well. The relevance for nuclear test monitoring is that acoustic signal travel-time errors translate directly into source location uncertainty, so it is necessary to determine how well travel times can be predicted from the Levitus database (Levitus, 1994), which is based on long-term averages. The ability of the IMS to estimate source locations within the Comprehensive Nuclear Test-Ban Treaty (CTBT) limit has been assessed for most of the world's oceans. To date, however, there had not been sufficient ground-truth data available to assess IMS location capabilities for the southern ocean.

The calibration shots were conducted over a period of three days in December 2006, so we obtained essentially a snapshot of propagation through the ACZ. Analysis of our signals will allow us to document the travel-times and transmission losses for the corresponding structure, to quantify travel-time errors associated with limited accuracy in ACZ models, and to characterize how well an unknown event in the southern ocean could be located. Other objectives are to determine how propagation through the ACZ affects signal strength and how source depth affects the transmission loss and travel times for source within the ACZ

RESEARCH ACCOMPLISHED

The Research Cruise

 Research Vessel Ice Breaker (RVIB) Nathanial B. Palmer departed Lyttleton, New Zealand, on 22 December 2006 (local time) and began a transit line toward the Adare Basin, the research area in the NW Ross Sea, for the main project on which our experiment piggybacked. The hydroacoustic project was conducted along the transit line during the first week of the cruise. Permission had been granted to conduct calibration shots in New Zealand waters, but no unblocked acoustic paths to the operational IMS stations were available during daylight hours, the latter being a requirement of our marine mammal mitigation procedure. From the southern edge of Campbell Plateau to ~63°S, hydroacoustic stations were occupied twice a day, approximately 120 nm apart.

Each station comprised a series of activities: The first to begin was the marine mammal watch (1 hr before expected shot time). After half an hour a sonobuoy was launched to allow mammal sound monitoring. An Expendable Bathy-Thermograph (XBT) was launched and ship speed slowed (to 1-2 kts) just before station occupation. An over-the-side hydrophone was deployed, and recording started. Signal underwater sound (SUS) charges were dropped at about 5 minute intervals at each station. When shots were completed, ship transit at full speed was resumed.

Marine Mammal Watch.
Before and throughout each acoustic station, marine mammal observers did visual checks in all directions for any animals that might be in the vicinity, particularly within the safety zone for the calibration shots. A safety zone size of 1 km was used for all 4-lb charges (~160 dB re µPa energy density at this range from the shot). A marine mammal observer participated in the watch for each station. About 30 minutes before the planned shots, a surplus US Navy sonobuoy was launched, and a marine mammal observer listened for marine mammals on the headphones. Two scientists participated in the marine mammal watch (~1.5 hours total).

SUS Depth Charges.
The SUS charges employed were MK59-mod1a with a 4-lb main charge. These were manufactured at the Indian Head Division (IHDIV) with firing depths of 1000', 1500', and 2000'. Transport from Yorktown, VA, to Christchurch was arranged by the US Navy via a military training flight from McChord Air Force Base. Transshipment approval from New Zealand Environmental Risk Management Authority was obtained, and temporary storage of the SUS was arranged at a local quarry storage facility.

At each hydroacoustic station, multiple SUS charges were hand-dropped one at a time from the helo deck. A single drop was done for each depth setting, starting from shallowest and working to deepest. The shot locations are listed in Table 1; their basic paths to the IMS hydrophones are shown in Figure 1. At stations A1-A4, a single charge was dropped for each trigger depth. The intent at A1 was to deploy one 1000' charge and two 1500' charges, since water depth was only 800 m. Interestingly the signal from the 3rd drop has charge-seafloor range and bubble pulse frequency closer to what would be expected for a 2000' firing. This suggests, contrary to the SUS manual, that occasionally firing depth can be off the trigger setting by up to 150 m. For the 1000' charge at A1, the seafloor reverberation and bubble frequency was within 25 m of expected trigger depths. The period of the bubble pulse for all subsequent stations was within the range expected for each nominal trigger depth and an uncertainty of ~35 m, as the SUS manual reports.

At stations A2-A4 and A6, drops were done for each depth setting (1000', 1500', and 2000'). At station A5 only 2 drops were done with the 2nd having two 1500'-triggered charges taped together, for an 8-lb total charge. The larger charge was chosen after onshore monitoring of IMS recordings by Catherine de Groot-Hedlin indicated that none of the signals from A2 had been detected at the Cape Leeuwin hydrophones. As later became clear, topographic blockage, not insufficient signal strength. was the culprit. At station A6, four drops were done with 2 being set for 1500' detonation. A combination of 4-lb, 8-lb, and 12-lb total charges were deployed at this last station.

Table 1: Shot locations and times

| Station SUS (ft-lb)	jday	shot time (Z)	shot depth [m]	latitude (S)	longitude (E)
A1					
S1000-4	359	4:06:01.79	330	53.850	171.7252
S1500-4	359	4:12:34.18	523	53.853	171.7258
S1500-4	359	4:18:43.70	614	53.856	171.7262
A2					
S1000-4	359	17:39:48.73	300	55.9788	171.7180
S1500-4	359	17:46:21.52	460	55.9794	171.7204
S2000-4	359	17:52:45.04	600	55.9798	171.7232
A3					
S1000-4	360	4:03:36.43	300	57.5648	171.7184
S1500-4	360	4:09:52.01	460	57.5674	171.7208
S2000-4	360	4:15:39.35	600	57.5698	171.7228
A4					
S1000-4	360	17:35:30	300	59.448	172.5763
S1500-4	360	17:41:40	460	59.449	172.5780
S2000-4	360	17:47:34	600	59.450	172.5804
A5					
S1000-4	361	4:01:32.95	300	60.9068	174.9546
S1500-8	361	4:08:33.52	460	60.9102	174.0356
A6					
S1000-4	361	17:31:03.03	300	62.7006	176.2032
S1500-8	361	17:39:10.25	460	62.7030	176.2038
S1500-12	361	17:47:43.37	460	62.7044	176.2062
S2000-12	361	17:56:06.04	600	62.7058	176.2090
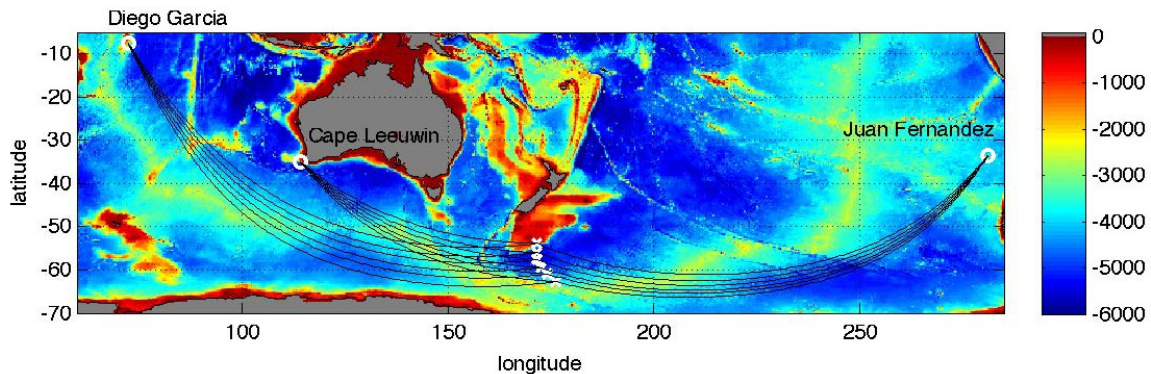
Figure 1. Map showing shot locations (x'es), IMS hydrophone station locations (circles), bathymetry, and geodesic paths from source to receiver. Stations are numbered A1 to A6 from north to south.

Near-Source Hydrophone.

A near-source hydrophone recording system was put together by Scripps Institution of Oceanography's (SIO's) Ocean Bottom Seismograph Instrument Pool personnel. This consisted of a data logger, a new 100 ft cable by Impulse, and a new HiTech HTI-90U hydrophone. A sample rate of 1000 Hz was used for single channel recording at the near-source hydrophone. The GPS time sync from the ship's system was fed into the data logger. Ship speed during the 20-30 minute station varied from ~1-2 kts. Signal-to-noise ratio (SNR) of the SUS shots on the near-source hydrophone was very good. Seafloor reverberation was recorded only at the shallowest station (A1, ~810 m); it was not evident in unfiltered data from the 3800-5400 m depths at the other stations.

Hydrophone depth was consistently shallower than hoped for (4-6 m instead of 10-15 m) due to the ship's forward motion and the relatively small weight (~4 kg) used to sink the hydrophone. Thus the recorded signal consists of a direct arrival plus an amplitude-reversed reflection from the air-sea interface. Destructive interference occurs at low frequencies, i.e., those for which the wavelength is greater than the hydrophone depth or an odd multiple of the hydrophone depth, since the wavefield at the hydrophone is the sum of the arrival plus its amplitude-reversed image. In retrospect, it was just as well that the hydrophone did not sink to greater depth, as that would have resulted in destructive interference at higher frequencies. As it was, destructive interference was significant mainly at f>150 Hz, i.e., beyond the passband at the IMS stations and at f<15 Hz, where SNRs of the signals recorded at the IMS stations were low anyway. The sea surface reflection cannot be completely separated from the source signature since only one hydrophone was used rather than a vertical array, as would have been optimal. The effect of the sea surface reflection is to introduce an error in the source spectrum estimates of about 4 dB, as discussed in the Data Analysis section.

IMS Hydrophone Station Recordings.

Before the cruise, we arranged to have IMS data from relevant hydroacoustic stations copied by the Air Force Technical Application Center (AFTAC) to an SIO workstation for the 10-day period that calibration shots were expected. There were 3 IMS stations with unblocked acoustic paths from the shots: Cape Leeuwin (H01), off SW Australia; Juan Fernandez (H03), off Chile; and Diego Garcia (H08). Crozet IMS hydrophones were all blocked by the Kerguelen plateau. Unfortunately, the southern Juan Fernandez station had not been operational since the end of 2005, and it was not fixed in time for this experiment. During the experiment Blackman alerted de Groot-Hedlin of upcoming shots and emailed approximate times/locations upon completion of each station. Time periods on either side of the predicted shot arrival times at the IMS stations were investigated at SIO, and a report on detections was e-mailed back to the ship.

Sonograms for shots recorded at the IMS hydrophone stations are shown in Figure 2. The transmission paths are not entirely free of topographic blockages; for most paths, there is some ridge or plateau that projects at least partway into the sound channel and strips off the highest order modes. None of the shots from A2 were recorded at Cape Leeuwin – apparently shallow features along the Macquarie Ridge that are not resolved in the current Sandwell and

Smith topography model scattered the energy; however, all other shots had good SNR in the 25-100 Hz band at Cape Leeuwin. Signals from A1 through A3 were detected at Juan Fernandez, at a distance of over 8000 km but were blocked by Juan Fernandez Island for shots further to the south. Conversely, signal transmission was poor to Diego Garcia for sites A1 and A2 and slightly better for subsequent shots to the south.
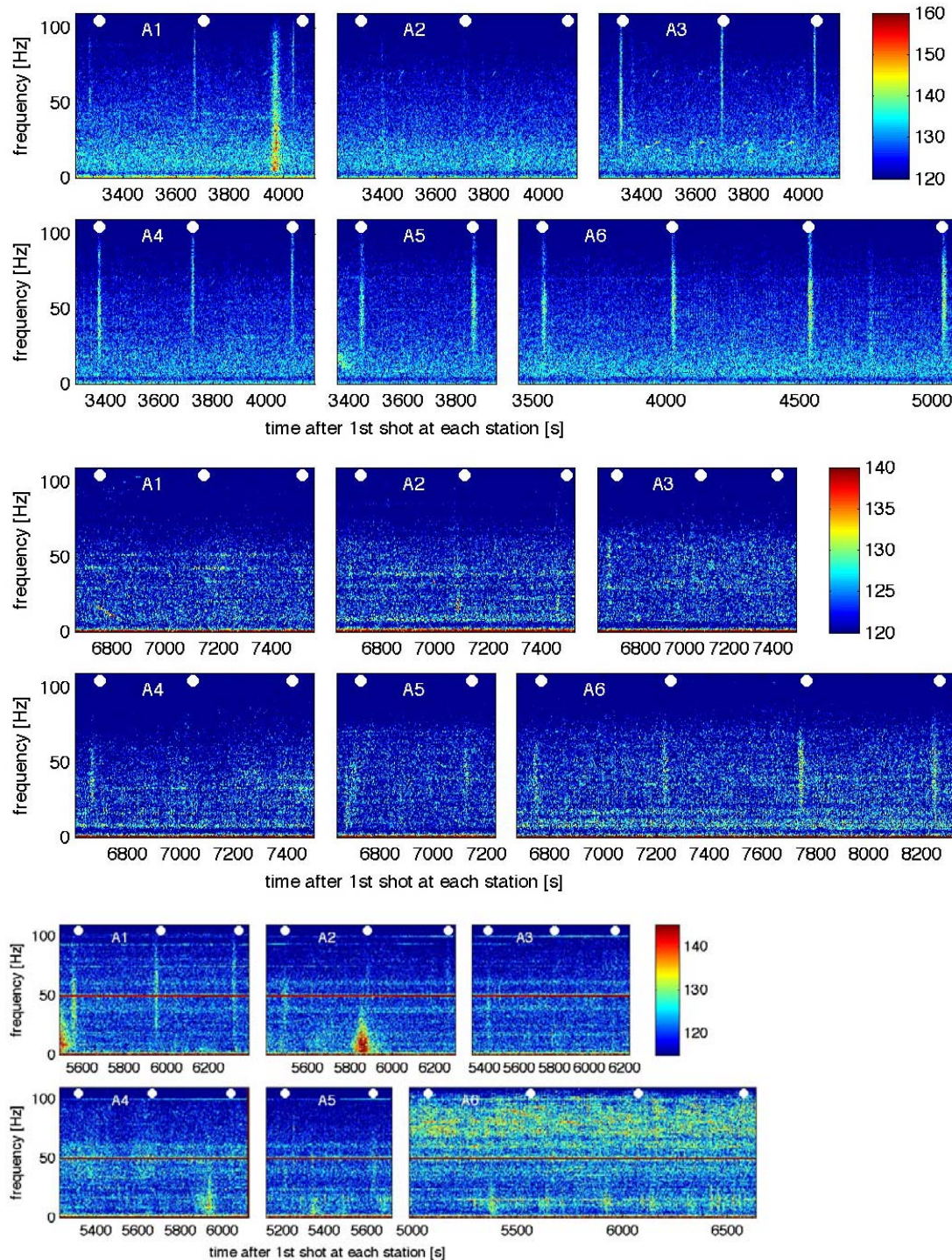

Figure 2. **Sonograms for shot recordings at Cape Leeuwin (H01W, top), Diego Garcia South (H08S, middle), and Juan Fernandez (H03N, bottom). Station is labeled (A1-A6) in each subpanel. The time axis for each sonogram is with respect to the first shot in the sequence. White dots indicate a first-order estimate of expected travel time.**

Data Analysis

We focus on two aspects of the analysis here: comparison of the observed and predicted travel times and estimation of the observed transmission losses as a function of frequency from source to receiver. The former relates to location estimates, the latter to yield estimates.

Transmission Losses

As previously discussed, a single near-source hydrophone at a depth of about 3-6 m was used to record the near-source pressure field. Thus, the recorded signal consists of a direct arrival plus a time-delayed, amplitude-reversed reflection from the air-sea interface, which may be represented in the time domain as

$$S_{rec}(t) = S_{true}(t) - R \times S_{true}(t - t_{echo}) = TF * S_{true}(t),$$

where TF is the transfer function representing the initial arrival and its echo and * denotes convolution. Convolution in the frequency domain is equivalent to multiplication in the time domain, so the power spectrum can be determined by dividing the power spectrum of the near-source recording by the power spectrum of the estimated transfer function. Fortunately, the zeros of the power spectrum of the transfer function lie either at very low frequencies for which the SNR was negligible and at f>125 Hz, i.e., at frequencies greater than the band of interest, since the instrument response of the IMS hydrophone stations drops off sharply at approximately f=100 Hz (Hanson and Bowman, 2005).
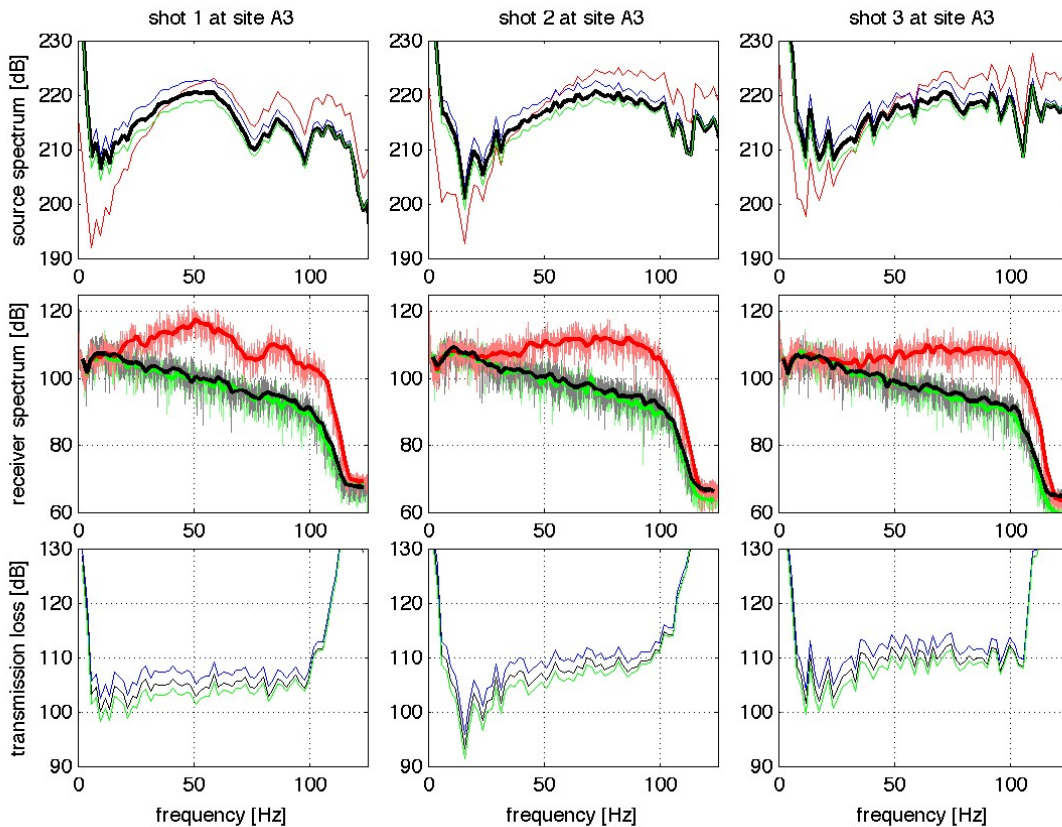

Figure 3. Source spectrum estimates (top row). raw (red) and corrected for echo from water surface, assuming time delays between initial pulse and reflected pulse of 4 ms (blue), 5 ms (black), and 6 ms (green). Power spectrum estimate for arrivals at Cape Leeuwin (middle row). Red lines are averaged signal spectrum, and green and black lines are power spectra for noise before and after the signal arrival, respectively. Heavy lines represent smoothed spectra. Transmission loss (bottom). Left to right – 4-lb shots at 300 m depth, 460 m depth, and 600 m depth. The blue, black, and green lines correspond to transmission losses derived from the source power spectral estimates of the same reflected-delay time assumption, keyed to color as in the top row panels.

However, deconvolution introduces some inaccuracy in the source spectrum estimate since one must know the precise delay time between the initial arrival and its echo, as well as the reflection coefficient off the surface—this is not exactly R = -1 for a rough sea surface. For these shots, cepstral analysis (not shown here) indicated a delay time of about 4-6 s. The source spectra for each shot conducted at site A3 (57.56°S, 171.72°E) are shown in the top row of Figure 3. All shots were 4-lb shots; shot 1 was detonated at 300 m, shot 2 at 460 m, and shot 3 at 600 m. The "zeros" in the source spectra are as predicted by bubble pulse theory; the first "zero" is at approximately 70 Hz for the 300 m shot, but for the deeper shots the first zeros are at frequencies greater than 100 Hz. The red lines indicate the uncorrected power spectra, while the blue, black, and green lines indicate the estimated power spectra corresponding to delays of 4 ms, 5 ms, and 6 ms, respectively. The difference between the source spectrum estimates – about 4 dB – is the error introduced by the necessity of having to deconvolve the sea surface reflection from the arrival.

Figure 3 also shows the power spectra for the waveforms recorded at Cape Leeuwin for the A3 shots, averaged over all three hydrophones (middle row), and the average source-receiver transmission losses for each shot. The results indicate that the transmissions are fairly uniform over the frequency range for which SNR>1. This is fortunate, as it means that the spectral scalloping associated with an explosive source may be observed at ocean basin scale distances. This result confirms computational predictions made using PE code modeling (Collins, 1993) indicating that transmission losses should be fairly uniform over the 30-100 Hz band for this source-receiver path. Also, note that the signal peak shifts toward lower frequencies for the shallower shots, with a peak at approximately 50 Hz for the 300 m shot. In addition, transmission losses are slightly lower for the shallower shots than for deeper shots.

Analysis of the remainder of the arrivals showed that the SNR was low at low frequencies for all source-receiver pairs; an unfortunate consequence is that the back azimuths cannot be computed accurately at the IMS hydrophone triplets. In theory, precise back azimuths can be computed by cross-correlating signals over narrow frequency bands and finding the best plane wave solution to the relative delay times. However, the degree of correlation decreases as the number of wavelengths between each hydrophone in the triplet increases. For the IMS stations, hydrophone separations are approximately 2 km within each triplet, thus the cross-correlations are most effective at frequencies of approximately 10 Hz or less. Thus the low SNR f < 20 Hz made this method infeasible. Determining back azimuths using travel time picks proved ineffective as well; the waveforms were emergent, thus travel times picks were accurate to only 0.5 seconds, which yielded very poor precision on computed azimuths.

Travel Times and Phase Duration
As a first approximation, travel times were computed assuming that hydroacoustic propagation follows geodesic paths from each source to receiver, i.e., the effects of lateral ray bending due to lateral variations in the sound speeds were ignored. The ocean sound speed profiles, derived from the Levitus database, were corrected for the effect of Earth curvature over these paths; this allows one to examine an arc path over the spherical Earth as a rectangular slice. Travel times and durations were then computed using group velocities corresponding to normal modes. Figure 4 shows an example of a travel time computation for mode 1 along a profile from site A1 to Juan Fernandez. As indicated, the axis of the sound channel shoals significantly toward the polar ocean and group velocities, especially for the lowest lower modes, vary significantly along the transmission path. The variation in group velocity along the path decreases at higher mode numbers. The effect of Earth curvature on total travel time is relatively insignificant: the travel time for the path shown in Figure 4 decreases by only about 0.3 seconds over a range of about 8200 km when Earth curvature is accounted for.

Our results also show that in most cases both the expected arrival time and duration can be predicted quite accurately using adiabatic normal mode theory. Figure 5 shows a sonogram and waveform of the recordings at Cape Leeuwin for the 12-lb shot at a depth of 460 m at station A6. Also shown are predicted arrival times for the first 20 modes at a source frequency of 40 Hz (white triangles). Travel times were computed as illustrated in Figure 4: a group velocity was computed for each of a number of points along a geodesic path from source to receiver, and the results were integrated to estimate the travel time. Higher order modes have higher average group velocities and thus arrive earlier than the mode 1 arrival – the one marked by the last triangle at the top of Figure 5. However, mode 1 is the most robust mode, i.e., the least susceptible to being stripped by bathymetry; this suggests that, for an underwater source, the time pick should be at the end of the waveform, rather than at the peak amplitude or peak frequency. The results shown in Figure 5 indicate that the duration of the arrival – about 18 seconds – agrees well with the degree of dispersion predicted using adiabatic mode theory for propagation along a geodesic path.
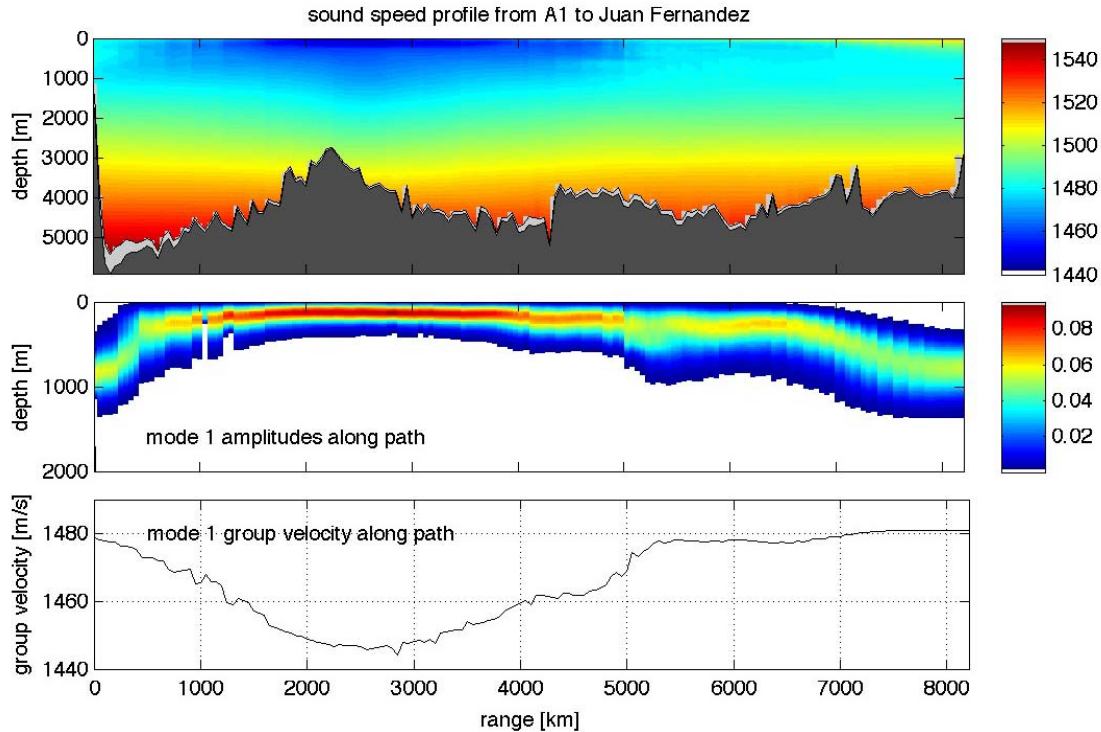
Figure 4. Top. Average winter sound speed profile along the source-receiver path, derived from the Levitus database, and corrected for Earth curvature. Sediment thickness (from Mooney et al., 1998) is indicated by the light gray zone. Center. Mode 1 amplitudes along the path for a source frequency of 40 Hz. Attenuation occurs where non-zero amplitudes intersect the bottom bathymetry, i.e., attenuation is negligible along this deep water path for mode 1. However, some scattering may take effect since transmission is surface limited over much of the path. Bottom. Group velocities along the travel path for mode 1 for a 40 Hz source. Group velocities are used to predict the acoustic travel time from source to receiver.
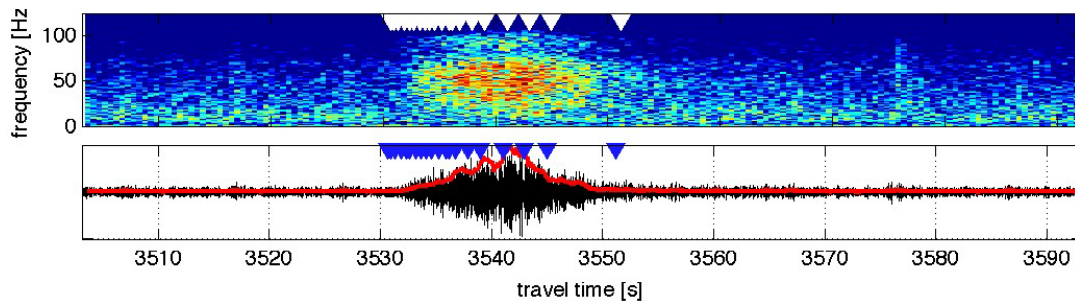

Figure 5. Sonogram and waveform for a recording at a single hydrophone at Cape Leeuwin for a 12-lb shot at a depth of 460 m at station A6. White (and blue) triangles show the expected arrival times for the first 20 modes, based on mean winter sound speed models and propagation along a geodesic travel path. Lateral ray-bending due to sharp velocity contrasts at the ACZ reduces the travel time by approximately 0.9 s for mode 1 - the last arrival.

Figure 6 shows the corresponding results for observations at Diego Garcia for the same shot. Predicted travel times for only 10 modes are shown here since the attenuation is predicted to be greater for this travel path. The waveform duration is again on the order of 18 seconds, as predicted by the computed mode arrival times. Arrivals for shots at stations A1 through A4 have durations on the order of 8-11 seconds, where observed, while stations A5 and A6 have

704

durations on the order of 18-20 s. That is, there is greater dispersion for sites further to the south within the polar ocean. The waveform durations at all stations were predictable using adiabatic normal mode theory and using winter sound speed profiles derived from the Levitus database.
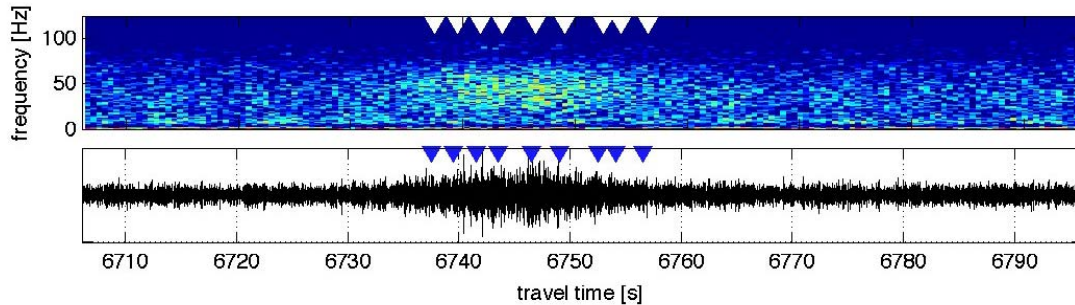

Figure 6. Sonogram and waveform for a recording at a single hydrophone at Diego Garcia South for a 12-lb shot at a depth of 460 m at station A6. White (and blue) triangles show the expected arrival times for the first 10 modes, based on mean winter sound speed models and propagation along a geodesic travel path. Lateral ray-bending due to sharp velocity contrasts at the ACZ reduces the travel time by approximately 0.9 s for mode 1.

Predicted arrival times for mode 1 agree with observations to within several seconds at these stations. Note these travel times are for propagation along the geodesic path; lateral ray-bending reduces the travel time by approximately 0.9 seconds for mode 1 at both Cape Leeuwin and Diego Garcia South. Figure 7 shows the lateral path deflections for paths from each shot site to each IMS hydrophone station, superimposed on a map of the group velocities. There is a significant increase in group velocities going from south to north across the Antarctic Convergence Zone for mode 1 as indicated, thus ray-bending is significant for mode 1. Ray-bending decreases the travel time to the Diego Garcia stations by as much as 5 seconds at station A3, by up to 3.9 s at Juan Fernandez, and by up to 2.2 s at Cape Leeuwin, as compared to propagation along a geodesic path. The contrast in group velocities across the ACZ decreases at higher modes; thus, ray-bending becomes less significant with increasing mode number.
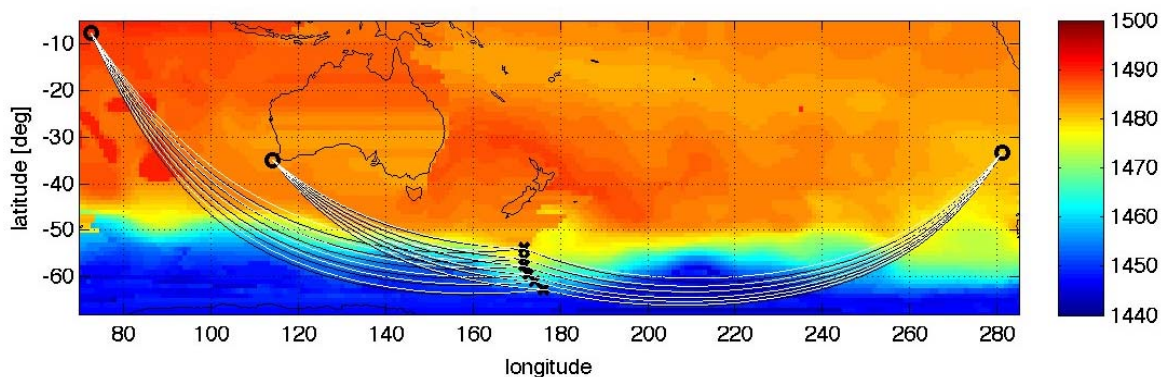

Figure 7. Lateral variation in group velocities causes a deflection of the propagation path from the geodesic; this effect was computed using the ray-bender code supplied in the hydrocam software (Farrell et al., 1996). Effect of lateral ray-bending from the December 2006 shots (labeled A1-A6) to the IMS hydrophone stations for mode 1 arrivals at a source frequency of 40 Hz. The black curves are geodesics; the white curves show the deflected ray paths corresponding to the minimum travel time paths. Group velocities were computed using average winter sound speed profiles and vary from approximately 1450 m/s (blue) to 1495 m/s (yellow). Lateral deflection has the effect of decreasing the travel time by several seconds for mode 1 and slightly less for higher order modes.

Both arrival times and waveform durations were predictable at all shot sites, to within 2 seconds —using adiabatic normal mode theory and using winter sound speed profiles derived from the Levitus database. This implies that location estimates should be accurate for sources observed at two or more stations. However, determinations of paths for shots near the boundary of the ACZ, between the colder waters to the south and warmer water to the north, are affected significantly by complexities in the shape of the time-varying boundary. Thus, temperature and sound speed profiles derived from the Levitus database, which is drawn from observations averaged over a long term, may produce somewhat less accurate predictions for near-boundary shot sites than for sites further to the south, well within the Antarctic circumpolar current, where discrepancies between local and mean velocities may average out.

CONCLUSIONS AND RECOMMENDATIONS

We have completed a relatively inexpensive experiment by piggybacking on a previously funded research cruise. We fired a series of test shots along a transit from Christchurch, New Zealand, to McMurdo station in the Antarctic, allowing us to test propagation characteristics across a range of polar front acoustic propagation paths. Most shots were detected at least one IMS station. Our main results to date are as follows:

- Highest SNR values were recorded for shots at 300 m depth, the shallowest depth tested.
- Observed transmission losses are fairly uniform as a function of frequency, in agreement with theoretical results provided by PE computations.
- There is significant variation in group velocities along the path, particularly at the lowest modes.
- Oceanographic gradients within the polar front alter the path of an acoustic wave, decreasing travel time by as much as 5 s, as compared to propagation along a geodesic path.
- Observed travel times and phase durations for sites well to the south of the ACZ boundary agree to within several seconds with theoretical results from adiabatic mode computations.
- Significant discrepancies in travel time are observed for sites nearest the ACZ boundary.

Comparison of observations with theoretical results suggests that further investigation of acoustic propagation for sites nearest the ACZ boundary is needed. We have thus proposed another research cruise to obtain more detailed measurements. Our new plan calls for several improvements to the previous experiment design. First, shots will be conducted at shallower depths than for our previous experiment to increase both the SNR and the width of the frequency band of the recorded signal. Second, we plan to deploy either a vertical hydrophone array or autonomous instruments near the source to more accurately estimate the source spectrum. Finally, we plan to do repeat SUS charges at a given depth at a single site; this would allow us to stack signals from a given depth, thereby increasing the SNR at the IMS stations and ensuring that marine mammals are not harmed.

REFERENCES

Collins, M.D. (1993). A split-step Padé solution for the parabolic equation method, *J. Acoust. Soc. Am*. 93: 1736–1742.

Dushaw, B. D. (1999). Inversion of multimegameter range acoustic data for ocean temperature. *IEEE J. Oceanic Engineering* 24: 215–223.

Farrell, T., K. LePage, and C. Barclay (1996). Users guide for the hydroacoustic coverage assessment model (hydroCAM), BBN Technical Memorandum W1273.

Hanson, J. A., and J. R. Bowman (2005). Dispersive and reflected tsunami signals from the 2004 Indian Ocean tsunami observed on hydrophones and seismic stations, *Geophys. Res. Lett.* 32: L17606, doi:10.1029/2005GL023783.

Levitus, S., *World Ocean Atlas* (1994). NOAA Atlas NESDIS 4, Washington D.C.